some broader vortex-like images (Fig. 2E) were observed. Forty images in the turbulent flame at $x/d = 50$ gave a most probable width of 2.1 mm with a broad range from 1.2 to 9.6 mm. The most probable width is smaller in the turbulent than in the laminar flame because of flame stretching due to increased shear. The wide range of measured turbulent flame zone widths may also be due to the reaction sheet not being perpendicular to the image plane or to overlapping of several different reaction zone sheets.

Figure 3 shows representative images from each of the flames at each of the positions investigated. The turbulent reaction zones observed at $x/d = 100$ and 150 differ qualitatively from the laminar, transitional, and even the $x/d = 50$ turbulent reaction zones; pockets appear that are not attached (at least in the imaged plane) to the rest of the reaction zone (see cover). In addition, the reaction zone sometimes does not extend continuously across the image, perhaps indicating breakup of the flame sheet.

The results reported here are qualitatively different from instantaneous flame fronts previously measured in premixed turbulent flames (*11*), where the instantaneous flame thicknesses were the same as the laminar premixed flame thicknesses (0.7 mm) and were independent of flame positions in accord with a "wrinkled laminar flame" model. Our measurements of nonpremixed turbulent flames indicate that (i) instantaneous flame thicknesses are considerably narrower than in laminar nonpremixed flames, (ii) flame thickness increases with downstream distance, and (iii) in some cases the flame sheet is apparently discontinuous.

The complex reaction zone structures that have been observed are in many ways similar to mixing zone structures in turbulent nonpremixed flames observed in Mie scattering studies (*9*). Such observations may help shed light on the importance of reaction zone and large-scale structures in understanding turbulent combustion and other reacting flow systems.

GEORGE KYCHAKOFF
ROBERT D. HOWE
RONALD K. HANSON
Department of Mechanical Engineering, Stanford University, Stanford, California 94305
MICHAEL C. DRAKE
ROBERT W. PITZ
MARSHALL LAPP*
C. MURRAY PENNEY
General Electric Research and Development Center, Schenectady, New York 12301

References and Notes

1. P. A. Libby and F. A. Williams, Eds., *Turbulent Reacting Flows* (Springer-Verlag, New York, 1980).
2. W. Kollmann, Ed., *Prediction Methods for Turbulent Flows* (McGraw-Hill, New York, 1980).
3. R. W. Bilger, *Combust. Flame* **26**, 115 (1976).
4. D. B. Spalding, *Proceedings of the 17th International Symposium on Combustion* (Combustion Institute, Pittsburgh, 1978), p. 431.
5. A. F. Ghoniem, A. J. Chorin, A. K. Oppenheim, *Philos. Trans. R. Soc. London Ser. A* **304**, 303 (1982).
6. A. K. Oppenheim and A. F. Ghoniem, *AIAA Pap. 83-0470* (1983).
7. M. B. Long, B. T. Chu, R. K. Chang, *AIAA J.* **19**, 1151 (1981).
8. M. B. Long and B. T. Chu, *ibid.*, p. 1158.
9. A. J. R. Lysaght, R. W. Bilger, J. H. Kent, *Combust. Flame* **46**, 105 (1982).
10. M. B. Long, D. Fourgette, M. C. Escoda, C. Layne, *Opt. Lett.* **8**, 244 (1983).
11. S. Rajan, J. R. Smith, G. D. Rambach, *West. States Sect. Combust. Inst. Pap. 82-88* (1982).
12. M. C. Escoda and M. B. Long, *AIAA J.* **21**, 81 (1983).
13. M. Alden, H. Edner, G. Holmsted, S. Svanberg, T. Hogberg, *Appl. Opt.* **21**, 1236 (1982).
14. M. J. Dyer and D. R. Crosley, *Opt. Lett.* **7**, 382 (1982).
15. G. Kychakoff, R. D. Howe, R. K. Hanson, J. C. McDaniel, *Appl. Opt.* **21**, 3225 (1982).
16. G. Kychakoff, K. Knapp, R. D. Howe, R. K. Hanson, *AIAA J.* **22**, 153 (1984).
17. G. Kychakoff, R. D. Howe, R. K. Hanson, *Appl. Opt.*, in press.
18. R. P. Lucht, D. W. Sweeney, N. M. Laurendeau, M. C. Drake, M. Lapp, R. Pitz, *Opt. Lett.*, in press.
19. M. C. Drake, M. Lapp, C. M. Penney, S. Warshaw, B. W. Gerhold, *Proceedings of the 18th International Symposium on Combustion* (Combustion Institute, Pittsburgh, 1981), p. 1521.
20. M. C. Drake, R. W. Bilger, S. H. Starner, *Proceedings of the 19th International Symposium on Combustion* (Combustion Institute, Pittsburgh, 1982), p. 459.
21. M. C. Drake, M. Lapp, C. M. Penney, S. Warshaw, B. W. Gerhold, *AIAA Pap. 81-0103* (1981).
22. We are grateful to the Office of Naval Research (contract N00014-80-C-0882, NR-094-405) for supporting major portions of this work and to the Air Force Office of Scientific Research (contract F49620-80C-0091) for additional support of the Stanford group. We also acknowledge valuable interactions with F. Gouldin of Cornell University that helped to define the direction of this research and significant contributions to the experimental program by F. Haller and F. Haskell.
* Present address: Sandia National Laboratories, Livermore, Calif. 94550.

15 March 1983; accepted 25 August 1983

Turbidity Currents: Monitoring Their Occurrence and Movement with a Three-Dimensional Sensor Network

Abstract. *Detailed field data on the occurrence, flow pattern, and internal dynamics of both surge and continuous turbidity currents have been obtained with a three-dimensional array of optical and thermal sensors. The array, operated in a glacial lake in southeastern British Columbia, collected detailed information on the character of surge events with velocities reaching 110 centimeters per second and continuous underflows exceeding 90 centimeters per second. The findings (i) indicate that such currents are frequent events, occurring with density differences between the incoming stream water and the lake water as low as 0.19 kilogram per cubic meter of water; (ii) document the differences in the initiation and internal characteristics of the continuous and surge events; and (iii) support the concept of erosion by turbidity currents.*

The general laws describing the movement of turbidity currents have been the subject of considerable laboratory and theoretical study by geologists, engineers, and fluid dynamicists (*1*). Yet the collection of field data on such phenomena in differing environments has been limited to measurements over relatively short time spans and at only a few measurement points. As Normark (*2*) and others have pointed out, this lack of detailed field observations has left present theory with only limited empirical support. In an effort to provide more detailed field data, a three-dimensional array of optical and thermal sensors and a smaller system of current meters were installed and operated in a glacial lake in southeastern British Columbia during the summers of 1977 and 1978. The network provided both a continuous record of the occurrence of underflow events and surge events and data on the internal characteristics of the flows. To my knowledge, this work constitutes the first use of a three-dimensional network in the study of turbidity currents.

A glacial lake provides excellent opportunities for measuring turbidity currents because of the often high and rapidly fluctuating discharge and sediment loads associated with most glacial meltwater systems and because of the diminished thermal, biological, and pollutant effects. The particular lake selected for monitoring is in the central Purcell range at 51°N, 116°W. Its relatively simple hydrologic setting, with only one main glacially fed stream entering it, gently varying lake-bottom topography, shallow mean depth of 5 m, and small size of less than 0.5 km^2 made it an ideal natural laboratory for the study of turbidity currents (Fig. 1).

The primary instrument network was designed to monitor the passage of underflow currents down the foreslope and into the lake. It consisted of 27 sensor packages organized in a 3 by 3 by 3 array (Fig. 1). Each package includes a tem-

perature sensor, a photo-optical turbidity sensor, and a suspended sediment sampler. The temperature sensors were precision thermilinear thermistors. The underwater optical sensors, designed by Weirich, provide a continuous measure of the concentration of suspended sediment in the lake. The sensors are double-beam transmissometer units that use matched photovoltaic cells, band-pass filters, and constant-voltage light sources.

In the field deployment, three sensor packages were mounted vertically on a rigid frame. This arrangement allowed the units at each station to be raised and lowered while maintaining the vertical spacing between packages. Nine such frames constituted the main array. Three current meters were also incorporated into the array. Data from the entire underwater system (some 90 channels) were transmitted to shore through some 7000 m of cable and recorded on a variety of data-recording devices, including a Fluke Summa II data-logging system with a Kennedy incremental tape recorder. The data logger was programmed for scan rates of 15 channels per second with intervals ranging from 10 minutes between scans to continuous scanning, depending upon the level of activity in the lake. In addition, some 20 channels of data from an array of hydrologic and climatic instruments located around the lake were also recorded by the logging system.

The data obtained from the sensor network indicate that density underflows are frequent in such environments. The general daily pattern for such events consisted of a morning underflow followed by a lull in activity, some occasional early afternoon and frequent late afternoon and early evening underflows, and a falling off of activity in the late evening. Careful determination of density differences between the incoming stream water and the lake water (taking into account the amounts of dissolved and suspended material and thermal data) indicated that underflows can occur when the density difference is as low as 0.19 kg m^{-3} ($\pm$0.02 kg m^{-3}). When density values were below this level, no underflows were detected; this finding suggests that a threshold may exist at this value.

Data for 10 August 1978 are presented in Fig. 2 and 3 as examples of the types of results obtained. The current meter readings (Fig. 2) show velocity in both the *X* and the *Y* directions at station 1, line 2, at a depth of 0.50 m. Figure 3 gives the optical data for the same location and the data for a station farther from shore. These optical readings were corrected for the "background" level within the lake by using data from a multilevel sensor station located in the lake beyond the sensor grid in an area where underflows did not reach. On this particular day, two events were detected by the system: a continuous underflow in the morning lasting from 8:00 to 11:30 and an afternoon surge event starting at 14:07 and lasting some 13 minutes. Both followed similar routes moving 20 m down a gradient of 0.227, and then 40 m down a gradient of 0.037 before moving out into the central portion of the lake. However, they differed markedly in character.

The continuous underflow began slowly with a gradual increase in the density of the incoming glacial meltwater. This gradual density increase was due to the combined effect of the warming of incoming water from 2.5°C toward the thermal maximum density of 4°C and a

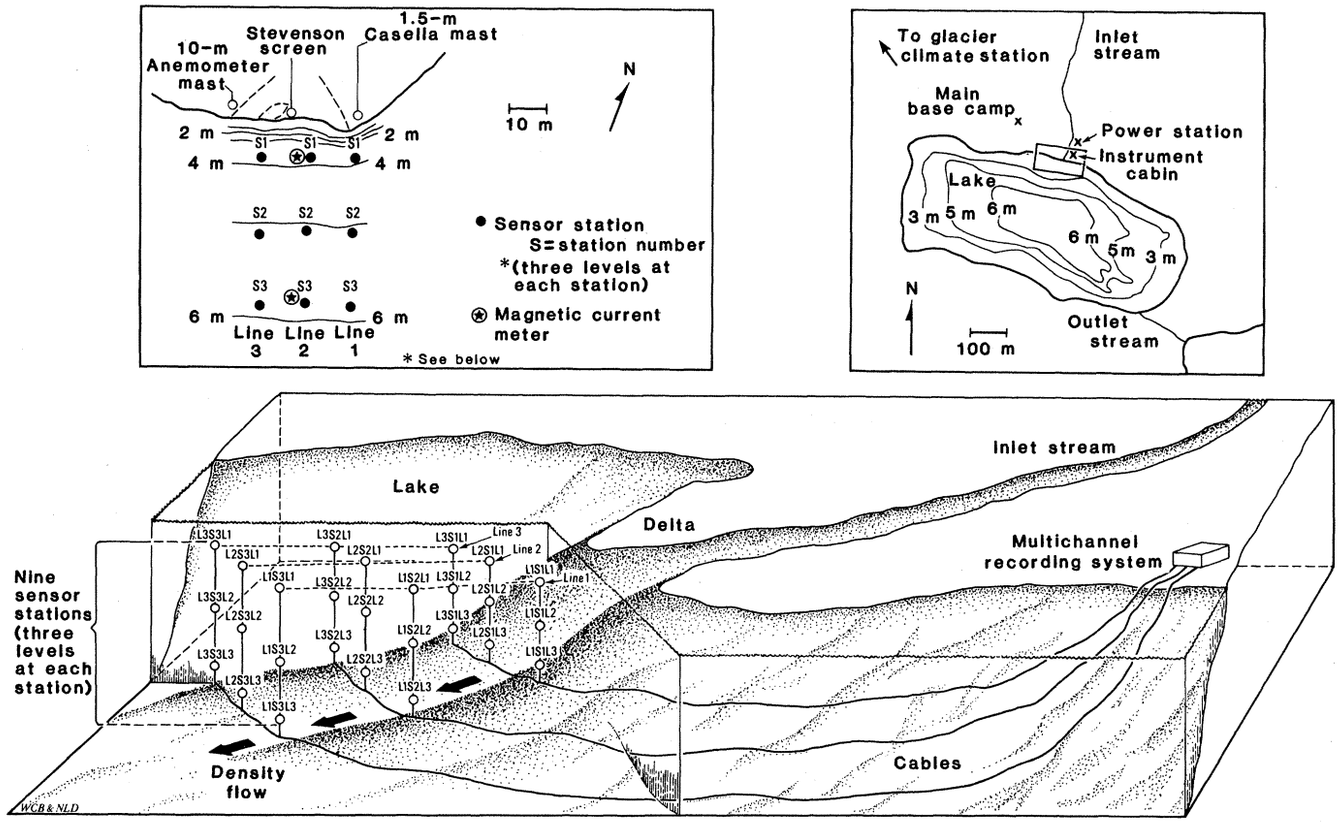

Fig. 1. The three-dimensional underwater sensor network. The actual locations of each line and individual stations as well as the level of each package can be altered to suit changing conditions in the lake. The locations of the main base station, instrument cabin, and hydroelectric station supplying power for the instrumentation network are indicated on the inset. The detailed plan view of the underwater network also indicates the location of some of the climatic monitoring equipment, specifically a 10-m anemometer mast, a Casella anemometer, and a Stevenson-type weather shelter containing temperature and relative-humidity monitors.

density increase caused by an increase in the concentration of the suspended sediment load. Although the onset of the underflow was detected at 8:00, the peak velocity of 91 cm sec^{-1} was not reached until about 10:20 when the density difference reached its maximum of 0.25 kg m^{-3}. As the morning progressed, the stream temperature rose above the thermal maximum density; thus the density of the input water decreased, and the density difference declined. By 11:30 the density difference between input and lake had dropped below 0.19 kg m^{-3} and the underflow had ended. The thickness of flow during the event, as indicated by optical sensor data, was at least 1.5 m. On the basis of temperature profile data, isothermal lake conditions prevailed before, during, and after the event. The direction of movement of the underflow through the sensor network was quite clear. Stations in line 1 showed no sign of it, while all stations in lines 2 and 3 showed elevated sediment concentrations for the entire period of the event.

The afternoon surge event was quite different. It began rapidly, reaching a velocity of 85 cm sec^{-1} within 1 minute of onset. Pulsating flow in the range of 50 to 110 cm sec^{-1} then ensued until the event ended abruptly 13 minutes later.

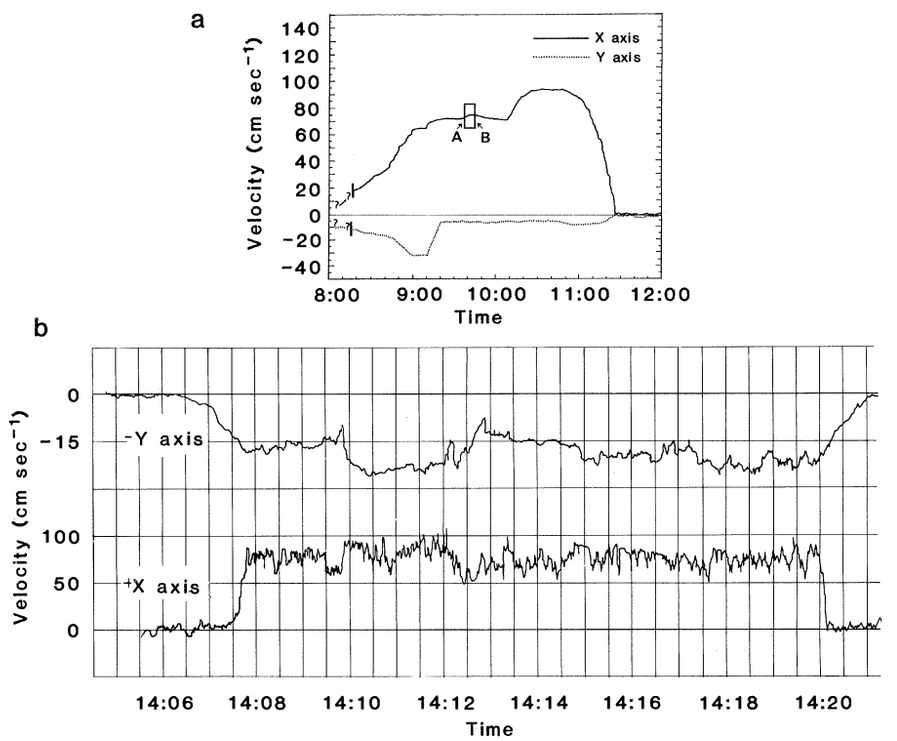

Fig. 2. (a) Electromagnetic current meter record at station 1, line 2, of continuous underflow during the morning of 10 August 1978. Velocity on both the *X* (horizontal) and *Y* (vertical) axes is indicated. A positive velocity on the *X* axis indicates lakeward motion, and a negative velocity on the axis indicates bottomward (sinking) motion. (b) Electromagnetic current meter record for the same unit on the afternoon of 10 August 1978, showing the occurrence of the surge event.

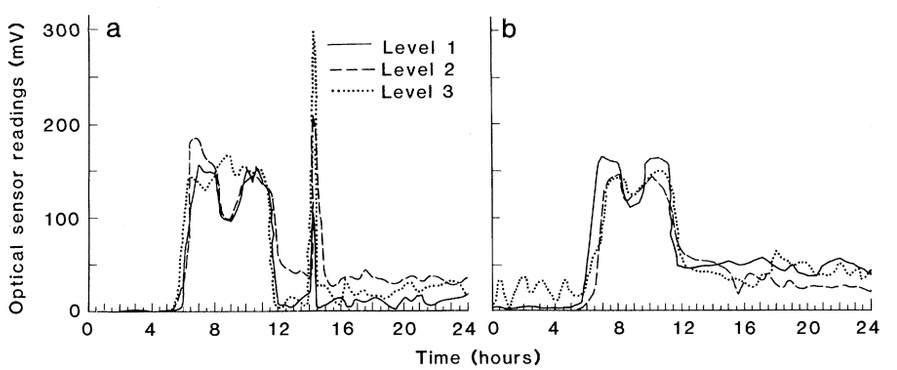

Fig. 3. (a) Optical readings from station 1, line 2, for all three levels on 10 August 1978, showing the data for both the morning underflow event and the afternoon surge. (b) Optical readings from station 2, line 3, for all three levels on 10 August 1978. The occurrence of the morning continuous underflow is clearly indicated.

Optical sensors indicated a flow thickness of 1.5 m. Although there had been no rapid change in discharge or temperature before onset, an abrupt increase of the suspended load in the incoming stream from 260 to 550 mg $liter^{-1}$ at 14:07 was recorded by an optical sensor in the stream. The end of the event coincided with a decline of sediment concentration of 550 to 280 mg $liter^{-1}$ at this input. The most likely source of the sediment was a slumping of material from the stream bank. This surge event was detected only at all three stations of line 2 and at station 3 of line 3 but not elsewhere. The flow therefore moved through the middle of the network before spreading toward the right-hand part of the grid.

Although earlier stratigraphic (*3*) and the process studies (*4*) have documented the existence and general characteristics of density underflows in glacial and associated environments, detailed continuous and direct field documentation has not been available before. The results of this study indicate (i) a threshold density difference for the occurrence of the underflows of 0.19 kg m^{-3}, (ii) differences in the initiation processes of underflows and channel surge events, and (iii) sharply contracting internal characteristics of the two types of currents.

The velocity data are also of considerable significance. Although velocities were measured 0.5 m above the bed, extrapolation of the velocity profile from this level down to the bed suggests bottom velocities that are above the threshold values required for the erosion of finer-grained materials. Further support for erosion of sediment comes from lake-bottom cores in mid-lake areas several hundred meters from the delta area; these cores contain coarse sand–sized (more than 1.00 mm) materials. Calculation of the flow velocities required to move such materials [based on Bagnold's autosuspension criteria (*5*)] indicate bottom velocities exceeding 28 cm sec^{-1}. In addition to grain-size data, stratigraphic and structural data also indicate erosional activity.

Such detailed and integrated information on distinctions between surge and continuous events, flow and internal characteristics, and the resulting deposits is important in furthering our understanding of the frequency and the erosional and transport capabilities of turbidity currents. Results from such work also have a direct bearing on lake, reservoir, and harbor sedimentation problems including sediment distribution patterns, overall sediment budgets, water clarity, and calculations of reservoir life expectancies. The use of multidimensional, si-

multaneous, spatial sensor arrays, such as the one described here, in conjunction with detailed process and stratigraphic studies of lacustrine environments, should provide such information and improve our understanding of the general laws of motion governing density currents and their deposits.

FRANK H. WEIRICH
Department of Geography, University of California, Los Angeles 90024

References and Notes

1. General summaries of studies undertaken may be found in: V. A. Vanoni, Ed., *Sedimentation Engineering* (Report 54, American Society of Civil Engineers, New York, 1975), pp. 278–285; G. V. Middleton and M. A. Hampton, in *Marine Sediment Transport and Environmental Management*, D. J. Stanley and D. J. P. Swift, Eds. (Wiley, New York, 1976), pp. 197–218; J. S. Simpson, *Annu. Rev. Fluid Mech* **14**, 213 (1982); W. E. Galloway and D. K. Hobday, *Terrigenous Clastic Depositional Systems* (Springer-Verlag, New York, 1983), pp. 168–175 and 185–201; J. R. L. Allen, *Sedimentary Structures: Their Character and Physical Basis*, vol. 1, *Developments in Sedimentology 30A* (Elsevier, New York, 1982), pp. 47–56.
2. W. R. Normark, *Bull. Am. Assoc. Pet. Geol.* **62**, 549 (1978).
3. S. D. Ludlam, *Limnol. Oceanogr.* **12**, 618 (1967); F. P. Agterberg and I. Banerjee, *Can. J. Earth Sci.* **6**, 625 (1969); I Banerjee, *Geol. Surv. Can. Bull.* (Part A) **226**, 1 (1974); S. D. Ludlam, *Limnol. Oceanogr.* **19**, 656 (1974); D. Mankiewicz, *J. Sediment. Petrol.* **45**, 462 (1975); S. S. Harrison, *ibid.* **43**, 738 (1975); G. M. Ashley, *Soc. Econ. Paleontol. Mineral. Spec. Publ. 23* (1975), p. 304; W. H. Theakstone, *Sedimentology* **23**, 671 (1976); A. Lambert and K. J. Hsu, *ibid.* **26**, 453 (1979); R. A. Pickrill and J. Irwin, *ibid.* **30**, 63 (1983).
4. T. C. Gustavson, *Soc. Econ. Paleontol. Mineral. Spec. Publ. 23* (1975), pp. 249–263; A. M. Lambert, K. R. Kelts, N. F. Marshall, *Sedimentology* **23**, 87 (1976); N. D. Smith, *Can. J. Earth Sci.* **15**, 741 (1978); M. Sturm and A. Matter, in *Modern and Ancient Lake Sediments*, A. Matter and M. E. Tucker, Eds. (Special Publication No. 2, International Association of Sedimentologists, Liége, Belgium, 1978), pp. 147–168; R. Gilbert and J. Shaw, *Can. J. Earth Sci.* **18**, 81 (1981); N. D. Smith, *Arct. Alp. Res.* **13**, 75 (1981); J. Irwin and R. A. Pickrill, *N.Z. J. Mar. Freshwater Res.* **16**, 189 (1982).
5. W. R. Normark and F. H. Dickson, *Sedimentology* **23**, 815 (1976).
6. This work was funded by the National Research Council of Canada and the Canadian Department of Energy, Mines, and Resources. The loan of equipment by D. C. Ford and J. A. Davies of the Department of Geography at McMaster University; B. Goodison of the Canadian Atmospheric Environment Service; the Environmental Institute of the University of Toronto; and the Department of Geography of the University of Toronto is gratefully acknowledged. The support and encouragement of A. V. Jopling of the Department of Geography of the University of Toronto was crucial to the conduct of this work.

17 February 1983; accepted 10 February 1984

Congruent Paleomagnetic and Archeomagnetic Records from the Western United States: A.D. 750 to 1450

Abstract. *Two independently dated, high-resolution paleomagnetic records, one lacustrine and one archeological, record the passage across western North America of the same nondipole feature of the geomagnetic field during the time interval from A.D. 750 to 1450. Although these sequences indicate that correlation between paleomagnetic and archeomagnetic records is feasible under certain conditions, differences between the records underscore the difficulty of dating accurately an archeological site by correlation of a single archeomagnetic direction with a secular variation curve.*

Since the first paleomagnetic measurements of varved sediments from western New England were reported (*1*), the study of fine-grained lacustrine sediments has held the promise of providing long, continuous histories of the geomagnetic field and, eventually, a master curve to which shorter archeomagnetic records could be compared. It has also been suggested that the age of an undated archeological site or lava flow might be determined by correlating its paleomagnetic direction to a master curve of secular variation. However, the correspondence between paleomagnetic features observed in lacustrine sediments and contemporaneous archeomagnetic records has been disappointing; only the broadest trends in lacustrine records have been correlated to the archeomagnetic data (*2, 3*).

We have compared two independently dated, high-resolution paleomagnetic records from western North America, one lacustrine and one archeological, and have found that they contain the same nondipole feature of the geomagnetic field during a 700-year interval. The lacustrine record is from Fish Lake, a small lake in Steens Mountain of southeastern Oregon. The record is part of a 8.93-m composite section composed of nine overlapping 10-cm diameter cores representing a total length of 16 m and spanning the last 13,000 radiocarbon years before the present (B.P.). The presence of six tephra layers and other thin, distinctive bands allowed us to align the overlapping segments of different cores with an uncertainty of less than 0.3 cm. Age control for the composite section came from 18 radiocarbon dates from the Fish Lake cores as well as 19 radiocarbon dates from two nearby lakes containing the same tephra layers (*4*). Two of these tephra layers are from Mount Mazama (Crater Lake) Oregon (*5, 6*).

Core samples were collected in plastic boxes (2.5 by 2.5 by 1.8 cm) which were placed as close together as possible to obtain a nearly continuous record. Each box was fully oriented with respect to the axis of the core segment. Magnetic analyses indicated that the magnetic carrier was pseudo–single-domain magnetite with no hematitic component. This was not surprising because most detritus coming into Fish Lake is derived from Miocene basalt. Upon alternating field demagnetization the paleomagnetic directions were found to be extremely stable, and the intensities had median destructive fields of 200 oersteds.

The declination record from the two core segments that span the interval from 450 years B.P. to 3500 years B.P. (A.D. 1450 to 1950 B.C.) is shown in Fig. 1. Unlike many other paleomagnetic records from lake sediments, the Fish Lake record has low scatter and a high degree of serial correlation within each core as well as excellent agreement between the corresponding segments of different cores. Although the cores were not azimuthally oriented, the overlap and precise stratigraphic correlation between the cores made it possible to align them, one with another, to obtain a single (unoriented) composite record. The absolute orientation of this composite record was then determined by matching the declination at the level of the upper of the two Mazama tephras in the composite core with the declination of the corresponding Mazama tephra measured in the field at various sites in Oregon (*7*). Various checks for consistency showed that the cores had penetrated the sediment vertically and had not twisted during penetration.

Comparison of the inclination at the level of the upper Mazama tephra in the composite section with the inclination measured in the field as well as comparison of the inclination at the top of the core with the corresponding inclination determined from historical records showed that there was an inclination error in the lake sediments. From observations of sediment grain size and the absence of apparent bioturbation, this error was to be expected (*8*), and the composite record was corrected for it. The data were then combined and smoothed by a Gaussian weighting function corresponding to an 80-year moving "window" (*9*). The virtual geomagnetic poles (VGP's) corresponding to the smoothed and corrected data for the time interval A.D. 600 to 1450 are shown in Fig. 2A.

The archeomagnetic record for the interval A.D. 750 to 1450 was developed by Sternberg from archeological sites in the southwestern United States (*10*). His sequence is based on 73 independently